



HAL
open science

Multiple interaction and localization phenomenon in postbuckling of compressed thin-walled members

Angelo Luongo, Marcello Pignataro

► **To cite this version:**

Angelo Luongo, Marcello Pignataro. Multiple interaction and localization phenomenon in postbuckling of compressed thin-walled members. *AIAA Journal*, 1988, 26 (11), pp.1395-1402. hal-00804958

HAL Id: hal-00804958

<https://hal.science/hal-00804958>

Submitted on 26 Mar 2013

HAL is a multi-disciplinary open access archive for the deposit and dissemination of scientific research documents, whether they are published or not. The documents may come from teaching and research institutions in France or abroad, or from public or private research centers.

L'archive ouverte pluridisciplinaire **HAL**, est destinée au dépôt et à la diffusion de documents scientifiques de niveau recherche, publiés ou non, émanant des établissements d'enseignement et de recherche français ou étrangers, des laboratoires publics ou privés.

Multiple Interaction and Localization Phenomena in the Postbuckling of Compressed Thin-Walled Members

A. Luongo* and M. Pignataro†
University of Rome, Rome, Italy

In this paper, the effect of boundary conditions on multiple interactive buckling in thin-walled members under compression is analyzed by means of the general theory of stability. The total potential energy is expanded to up to third-order terms to investigate structures with asymmetric postbuckling behavior; initial geometric imperfections are taken into account. Under simplifying assumptions, the nonlinear equations governing the postcritical behavior reduce to a linear eigenvalue problem that is independent of the geometric and mechanical properties of the column and depends on the boundary conditions only. Localization of the buckling patterns is verified when a large number of local buckling modes occur simultaneously. A continuum representation, based on the substitution of the algebraic eigenvalue problem with a differential equation, is proposed.

I. Introduction

IN the past, many researchers gave a great deal of attention to the occurrence of simultaneous or nearly simultaneous buckling modes in elastic structures. This is due to the fact that structures with stable postbuckling behavior in correspondence with each of the single buckling modes may exhibit sensitivity to imperfection when two or more buckling modes interact.^{1,2} Following the pioneering work of Van der Neut³ and Koiter and Kuiken,⁴ a lot of work has been stimulated recently on this topic by the extensive use of high-strength materials in plate assemblages such as thin-walled members (TWM), where local and overall buckling modes are likely to occur simultaneously.⁵⁻¹² All this work, however, regards the interaction between one overall and one single local buckling mode (single interaction) and therefore is valid for moderately long members. For long members, an investigation of the interaction must necessarily take into account the presence of a greater number of local modes that occur under (nearly) the same critical stress (multiple interaction). This argument has been analyzed very recently in a few papers,^{13,14} where the postbuckling behavior of simply supported TWM under compression has been investigated.

In this work, the effect of multiple interaction on the postbuckling behavior of TWM under compression for various boundary conditions is analyzed. The analysis is based on the general theory of stability¹ by expanding the total potential energy up to third-order terms in order to investigate structures with asymmetric behavior. It is shown that, under suitable simplifying assumptions, it is possible to replace the nonlinear governing equations with a linear eigenvalue problem that is independent of the TWM geometric and mechanical properties and depends on boundary conditions only. The occurrence of a cluster of local buckling modes leads to a local deformation concentrated in one or more narrow bands of the beam axis. This phenomenon is known as "localization of the buckling patterns."¹⁵⁻¹⁷

All results can be justified on the basis of a continuum representation that can be applied when an infinite number of local buckling modes are interacting. This procedure is based on the replacement of the algebraic eigenvalue problem with a differential equation. A numerical example has been worked out on the postbuckling behavior of two stiffened panels with slender and stocky stiffeners under different boundary conditions.

II. Structural Model and Postbuckling Analysis

Let us consider the total potential energy of a plate of length ℓ , width b , and thickness t uniformly compressed by the stress N_x in the longitudinal direction x :

$$\begin{aligned} \Phi = & \frac{Et}{2(1-\nu^2)} \int_0^b \int_0^\ell \left[\varepsilon_x^2 + \varepsilon_y^2 + 2\nu\varepsilon_x\varepsilon_y + \frac{1}{2}(1-\nu)\gamma_{xy}^2 \right] dx dy \\ & + \frac{Et^3}{24(1-\nu^2)} \int_0^b \int_0^\ell \left[\chi_x^2 + \chi_y^2 + 2\nu\chi_x\chi_y \right. \\ & \left. + \frac{1}{2}(1-\nu)\chi_{xy}^2 \right] dx dy - \lambda \int_0^b N_x [u(0,y) - u(\ell,y)] dy \quad (1) \end{aligned}$$

Where E is the Young modulus, ν the Poisson ratio, and λ a load parameter. Let us assume for the strain measures the following expressions:

$$\begin{aligned} \varepsilon_x &= u_{,x} + \frac{1}{2}(v_{,x}^2 + w_{,x}^2), & \chi_x &= w_{,xx} \\ \varepsilon_y &= v_{,y} + \frac{1}{2}(u_{,y}^2 + w_{,y}^2), & \chi_y &= w_{,yy} \\ \gamma_{xy} &= u_{,y} + v_{,x} + w_{,x}w_{,y}, & \chi_{xy} &= 2w_{,xy} \end{aligned} \quad (2)$$

where u, v are the in-plane displacement components in the x, y directions, w is the lateral displacement, and a comma denotes differentiation with respect to the following variable.

By replacing Eqs. (2) into Eq. (1), the total potential energy in terms of the displacement gradients is derived. By considering the TWM as a plate assemblage, the total potential energy Φ is obtained by adding up all contributions from single plates. Explicit expressions of second- and third-order

*Associate Professor, Department of Structural and Geotechnical Engineering.

†Professor, Department of Structural and Geotechnical Engineering.

terms are furnished by

$$\begin{aligned}\Phi_2 = & \int_S \frac{Et}{2(1-\nu^2)} \left[u_{,x}^2 + v_{,y}^2 + 2\nu u_{,x}v_{,y} \right. \\ & \left. + \frac{1}{2}(1-\nu)(u_{,y} + v_{,x})^2 \right] dx dy \\ & + \int_S \frac{Et^3}{24(1-\nu^2)} \left[w_{,xx}^2 + w_{,yy}^2 + 2\nu w_{,xx}w_{,yy} \right. \\ & \left. + 2(1-\nu)w_{,xy}^2 \right] dx dy\end{aligned}\quad (3)$$

$$\begin{aligned}\Phi_3 = & \int_S \frac{Et}{2(1-\nu^2)} \{ u_{,x}(v_{,x}^2 + w_{,x}^2) + v_{,y}(u_{,y}^2 + w_{,y}^2) \\ & + \nu[u_{,x}(u_{,y}^2 + w_{,y}^2) + v_{,y}(v_{,x}^2 + w_{,x}^2)] \\ & + (1-\nu)(u_{,y} + v_{,x})w_{,xy} \} dx dy\end{aligned}\quad (4)$$

where S is the middle surface of the TWM. Fourth-order terms are not given, since it can be shown that, under suitable assumptions, they are not essential to the evaluation of the slope of the bifurcated paths.

If initial imperfections $\bar{u}, \bar{v}, \bar{w}$ are present, assuming the plates to be stress free in the unloaded state, the total potential energy Φ is modified by the addition of the extra contribution

$$\begin{aligned}\Psi = & -\frac{Et}{1-\nu^2} \int_S \left[u_{,x}\bar{u}_{,x} + \nu(u_{,x}\bar{v}_{,y} + \bar{u}_{,x}v_{,y}) + v_{,x}\bar{v}_{,y} \right. \\ & \left. + \frac{1-\nu}{2}(u_{,y} + v_{,x})(\bar{u}_{,y} + \bar{v}_{,x}) \right] dx dy \\ & - \frac{Et^3}{12(1-\nu^2)} \int_S [w_{,xx}\bar{w}_{,xx} + \nu(w_{,xx}\bar{w}_{,yy} + \bar{w}_{,xx}w_{,yy}) \\ & + w_{,yy}\bar{w}_{,yy} + 2(1-\nu)w_{,xy}\bar{w}_{,xy}] dx dy\end{aligned}\quad (5)$$

where only linear terms in the initial displacements have been retained.

For the analysis of the postbuckling behavior of the perfect structure, it is convenient to express the bifurcated path $v = v(\lambda)$ by a series expansion in terms of a parameter ξ :

$$\begin{aligned}\lambda = & \lambda_c + \lambda_1\xi + \dots \\ v = & v_1\xi + \frac{1}{2}v_2\xi^2 + \dots\end{aligned}\quad (6)$$

where v is a displacement vector measured from the fundamental path. The critical load λ_c and the buckling mode v_1 are determined by solving an eigenvalue problem, the remaining coefficients of Eqs. (6) being furnished by a second-order perturbation equation. In the case of r buckling modes v_{1i} associated with the same value λ_c , we have, for the general solution to the eigenvalue problem, $v_1 = v_i v_{1i}$, where the v_i are arbitrary constants and the summation convention with respect to repeated indices has been adopted. Without any loss in generality, these modes can be orthonormalized according to $\pi_2'' v_{1i} v_{1j} = \delta_{ij}$, where δ_{ij} is the Kronecker delta and π_2'' is the quadratic part of the elastic energy Φ . By requesting $\pi_2'' v_1^2 = 1$, the condition

$$v_i v_i = 1 \quad (7)$$

follows. The condition of solvability of the second-order perturbation equations leads to the nonlinear algebraic system in the unknowns v_i and λ_1 :

$$A_{ijk} v_j v_k + \lambda_1 B_{ik} v_i = 0 \quad (i, j, k = 1, \dots, r) \quad (8)$$

where

$$A_{ijk} = \Phi_c'' v_{1i} v_{1j} v_{1k} \quad (9a)$$

$$B_{ik} = 2\Phi_c'' v_{1i} v_{1k} \quad (9b)$$

a prime denoting a Frechet differentiation and $\Phi_c'' = [d\Phi''/d\lambda]_{\lambda_c}$. For the analysis of the imperfect structure, it is assumed for the initial displacements $\bar{u} = \xi \bar{u}^*$, where ξ is the amplitude and \bar{u}^* denotes the shape of the imperfections that is selected as $\bar{u}^* = v_i^* v_{1i}$, v_i^* being the set of coefficients corresponding to the postbuckling path of steepest descent of the perfect structure. In this case, by limiting ourselves to a third-order analysis, the snapping load is furnished by

$$\frac{\lambda_s}{\lambda_c} = 1 - 2\sqrt{\frac{\bar{\xi}\rho\lambda_1^*}{\lambda_c}} \quad (10)$$

for $\lambda_1^* > 0$ and $\rho\xi < 0$ or vice versa. In Eq. (10), $\lambda_1^* = \max\{\lambda_i\}$ is the largest slope coefficient, and

$$\rho = \tilde{\Psi}'_c(v_i^* v_{1i})^2 / \lambda_c \Phi_c''(v_i^* v_{1i})^2 \quad (11)$$

where a tilde denotes differentiation with respect to \bar{u} .

For a TWM, under the assumption of free transverse expansion, one obtains

$$A_{1jk} = \Phi_{3c}'' v_{1i} v_{1j} v_{1k}, \quad B_{ij} = -2\frac{\delta_{ij}}{\lambda_c}, \quad \rho = 1 \quad (12)$$

By eliminating ξ from Eqs. (6), the equilibrium path

$$\lambda/\lambda_c = 1 + \mu(v_P/h) \quad (13)$$

is obtained where

$$\mu = (\lambda_1/\lambda_c)(h/v_i^* v_{1i}^0) \quad (14)$$

v_P being a displacement component of a selected point P of the TWM, v_{1i}^0 the contribution to v_P from the i th buckling mode, and h a dimension of the cross section. The snapping load, Eq. (10), reduces to

$$\frac{\lambda_s}{\lambda_c} = 1 - 2\sqrt{-\mu \frac{\bar{u}_P}{h}} \quad (15)$$

where \bar{u}_P is a component of the displacement of the point P due to initial imperfections.

III. Multiple Interaction

Let us consider the case of multiple interaction between one overall mode, flexural (eulerian) or flexural-torsional, and m local modes characterized by n_2, n_3, \dots, n_{m+1} longitudinal half-waves with $n_j \geq 1$. The integers n_j belong to an interval with middle point n_0 to which corresponds the lowest local critical stress σ_{loc} coinciding with the overall critical stress. In our analysis, we assume that σ_{loc} remains constant inside the interval, so that the $m+1$ buckling modes occur simultaneously. The system of Eq. (8) consists in this case of $m+1$ nonlinear equations and $m+2$ unknowns $v_1, v_2, \dots, v_{m+1}, \lambda_1$ to which the normalization condition Eq. (7) must be added. A great computational effort is generally required to find all solutions of the system whose number is not known a priori, and, therefore, a simplified analysis appears to be desirable. To this end, we make a number of assumptions by distinguishing two approximation levels that permit us to achieve our purpose.

A. First Approximation Level

Two basic assumptions are made:

1) In the overall mode, the TWM buckles as a shear indeformable beam with free transverse expansion ($u_{,y} + v_{,x} = 0, v_{,y} = -vu_{,x}$), and the displacement field for the generic plate element is described by

$$u_1(x,y) = -a_1 U_1(y) f'(x) \quad (16a)$$

$$v_1(x,y) = a_1 U_1'(y) f(x) \quad (16b)$$

$$w_1(x,y) = a_1 W_1(y) f(x) \quad (16c)$$

where a prime denotes differentiation of a function with respect to the corresponding argument. Equations (16) are valid for any boundary condition if the overall buckling mode is Eulerian and only for particular boundary conditions for the flexural-torsional mode of open TWM.

2) In the local buckling modes, joints do not translate, so that only lateral displacements of the plate components are possible. The j th buckling mode is therefore represented by

$$u_j(x,y) = 0 \quad (17a)$$

$$v_j(x,y) = 0 \quad (17b)$$

$$w_j(x,y) = a_j W_j(y) \sin(n_j \pi x / \ell), \quad (j = 2, 3, \dots, m+1) \quad (17c)$$

Note that the displacement field of Eq. (17) is valid both for long TWM and for members restrained at the ends by flexible diaphragms inextensible in their own plane.

As a consequence of the first assumption, $A_{111} = 0$, and of the second, $A_{ijk} = 0$ for $i, j, k > 1$, since lateral displacements in Eq. (4) are always coupled with in-plane displacements. Besides, from assumptions 1) and 2) it follows that

$$A_{ijk} = \int_S Et(u_{1,x} w_{j,x} w_{k,x}) dS, \quad (j, k = 1, 2, \dots, m+1) \quad (18)$$

By replacing Eqs. (16) and (17) into Eq. (18) one gets

$$A_{1jk} = -E \frac{\pi^2}{\ell^2} a_1 a_j a_k n_j n_k c_{1jk} \int_{\mathcal{C}} U_1(y) W_j(y) W_k(y) t dy \quad (19)$$

\mathcal{C} being the cross-sectional middle line and

$$c_{1jk} = \int_0^{\ell} f''(x) \cos \frac{n_j \pi x}{\ell} \cos \frac{n_k \pi x}{\ell} dx \quad (20)$$

According to previous results, Eqs. (8) then simplify into

$$A_{1jk} v_j v_k - 2(\lambda_1 / \lambda_c) v_1 = 0 \quad (21)$$

$$A_{1jk} v_1 v_k - (\lambda_1 / \lambda_c) v_j = 0, \quad (j, k = 2, 3, \dots, m+1) \quad (22)$$

By posing

$$\eta = \lambda_1 / v_1 \lambda_c \quad (23)$$

Eqs. (22) read

$$(A_{1jk} - \delta_{jk} \eta) v_k = 0, \quad (j, k = 2, 3, \dots, m+1) \quad (24)$$

The system of Eqs. (24) represents a linear eigenvalue problem that furnishes m real eigenvalues, since matrix A_{1jk} is real and symmetric. By denoting with η_h the h th eigenvalue and with $v_k^{(h)}$ the corresponding eigenvector, the values of $v_1^{(h)}$

and $\lambda_1^{(h)}$ can be obtained by solving Eqs. (21) and (23):

$$v_1^{(h)} = \pm \frac{1}{\sqrt{3}} \quad (25a)$$

$$\frac{\lambda_1^{(h)}}{\lambda_c} = \pm \frac{\eta_h}{\sqrt{3}} \quad (25b)$$

The arbitrary constant of the eigenvector $v_k^{(h)}$ is determined, to within the sign, from the normalization condition Eq. (7), and, therefore, the $2m$ solutions $\lambda_1^{(h)}, v_1^{(h)}, \pm v_2^{(h)}, \dots, \pm v_{m+1}^{(h)}$ are obtained. Note that these solutions are independent of the sign of $\lambda_1^{(h)}, v_1^{(h)}$ furnished by Eqs. (25), and, therefore, they represent all bifurcated paths.

The coefficient v_1 furnished by Eqs. (25) shows that, along any bifurcated path, $1/3$ of the energy $\pi_1^2 v_1^2$ is associated with the overall mode and $2/3$ with the local modes, whatever the number m is. This derives from the fact that the buckling modes have been orthonormalized with respect to the quadratic operator π_2^2 .

B. Second Approximation Level

The previous analysis can be simplified if a further assumption is introduced:

3) The shape of the local critical mode in the cross-sectional plane is independent of the number of longitudinal half-waves.

This is true when the TWM plate components are simply supported along the longitudinal edges, and it is verified with good approximation for long plates with different boundary conditions and n_j not too far from n_0 . Under this assumption, it can be shown that, by using the normalization condition, the amplitude a_j of the local critical mode is proportional to $1/n_j$, according to

$$a_j^2 = \frac{1}{\lambda_c} \frac{2\ell}{n_j^2 \pi^2} (1/\int_{\mathcal{C}} W_\ell^2(y) t dy) \quad (26)$$

where $W_\ell(y)$ is the cross-sectional lateral deflection of any of the local modes. By virtue of Eq. (26), Eq. (19) can be written as

$$A_{1jk} = \mathcal{A} c_{1jk} \quad (27)$$

where

$$\mathcal{A} = -\frac{2Ea_1}{\lambda_c \ell} \int_{\mathcal{C}} U_1(y) W_\ell^2(y) t dy / \int_{\mathcal{C}} W_\ell^2(y) t dy \quad (28)$$

By denoting with $\eta_0 = \mathcal{A} c_{122}$ the eigenvalue for single interaction ($m = 1$), Eqs. (24) can be rewritten as

$$(c_{1jk}^* - \eta^* \delta_{jk}) v_k = 0 \quad (29)$$

where

$$\eta^* = \frac{\eta}{\eta_0} \quad (30a)$$

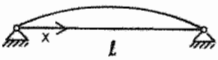

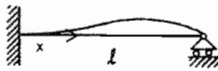
$$c_{1jk}^* = \frac{c_{1jk}}{c_{122}} \quad (30b)$$

In this analysis $\eta_0 \neq 0$ is assumed. Both this case and $\eta_0 = 0$ are treated in Ref. 18.

Equations (29) are independent of the geometrical and mechanical properties of the structure, and their solution depends on the boundary conditions and on the number m of local buckling modes only. The analysis of the problem at hand can therefore be carried out by determining η_0 from the problem of single interaction and multiplying the results by the amplifying factor η^* .

Within this approximation level, it can be shown¹⁸ that, for a large number of interacting buckling modes, matrix c_{1jk}^* is

Table 1 Coefficients for eigenvalue problem, Eq. (29), for various boundary conditions

	$f(x)$	c_{1jk}	c_{122}	c_{1jk}^*
	$\sin \pi \frac{x}{\ell}$	$-\frac{\pi}{\ell} \frac{1}{1 - (n_j - n_k)^2}$	$-\frac{\pi}{\ell}$	$\frac{1}{1 - (n_j - n_k)^2}$
	$1 - \cos \frac{2\pi x}{\ell}$	$(-1)^{n_j - n_k} \frac{\pi}{4\ell} \frac{1}{1 - 4(n_j - n_k)^2}$	$\frac{\pi}{4\ell}$	$\frac{(-1)^{n_j - n_k}}{1 - 4(n_j - n_k)^2}$
	$\frac{1}{2\pi} \left[\sin \alpha \frac{x}{\ell} - \alpha \cos \alpha \frac{x}{\ell} + \alpha \left(1 - \frac{x}{\ell} \right) \right]$	$\frac{\alpha^3}{4\pi^3 \ell} \frac{1 - (-1)^{n_j - n_k} / \cos \alpha}{(n_j - n_k)^2 - \alpha^2 / \pi^2}$	$\frac{4}{\pi \ell} \times \frac{1 - \cos \alpha}{\cos \alpha}$	$\frac{\alpha^2}{\pi^2} \frac{\cos \alpha}{1 - \cos \alpha} \times \frac{1 - (-1)^{n_j - n_k} / \cos \alpha}{(n_j - n_k)^2 - \alpha^2 / \pi^2}$
	$\alpha = 4.493$			

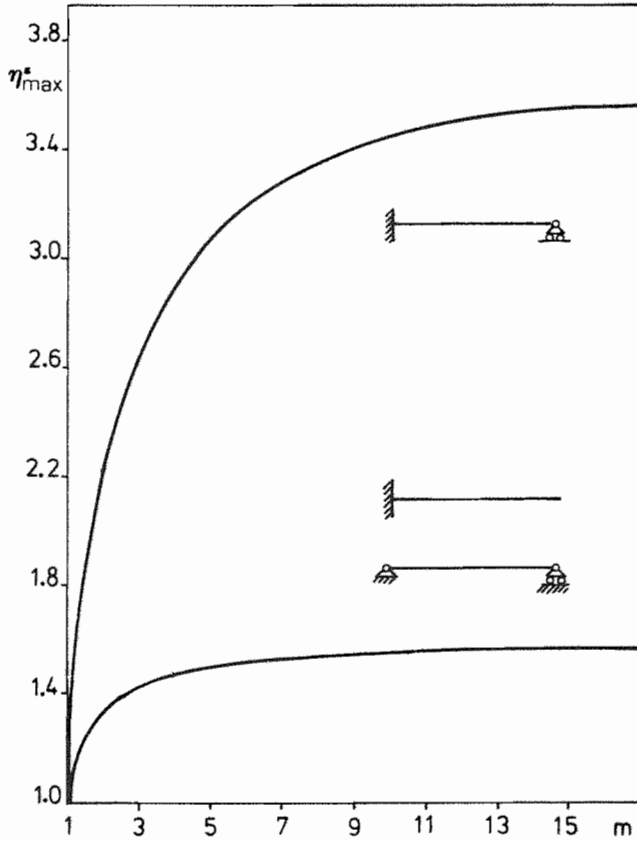


Fig. 1 Amplifying factor vs number of local buckling modes.

positive definite if $f''(x)$ maintains its sign in $[0, \ell]$, and it is indefinite if $f''(x)$ changes sign. Consequently, the eigenvalues η^* are all positive in the first case and have both signs in the second case. By remembering that $f''(x)$ is proportional to the bending moment of the overall buckling, one may conclude that if the bending moment is constant in sign, the beam global displacement always occurs in the same direction, whatever the shape of the local deformation; if the bending moment changes sign, then the direction of the global displacement depends on the local deformations.

IV. Effect of Boundary Conditions on Postbuckling

In a previous work,¹⁴ the effect of multiple interaction on the postbuckling of a simply supported beam at first and second approximation levels was investigated. In this section, our attention is focused on the effect of boundary conditions on the postcritical behavior of TWM within the framework of

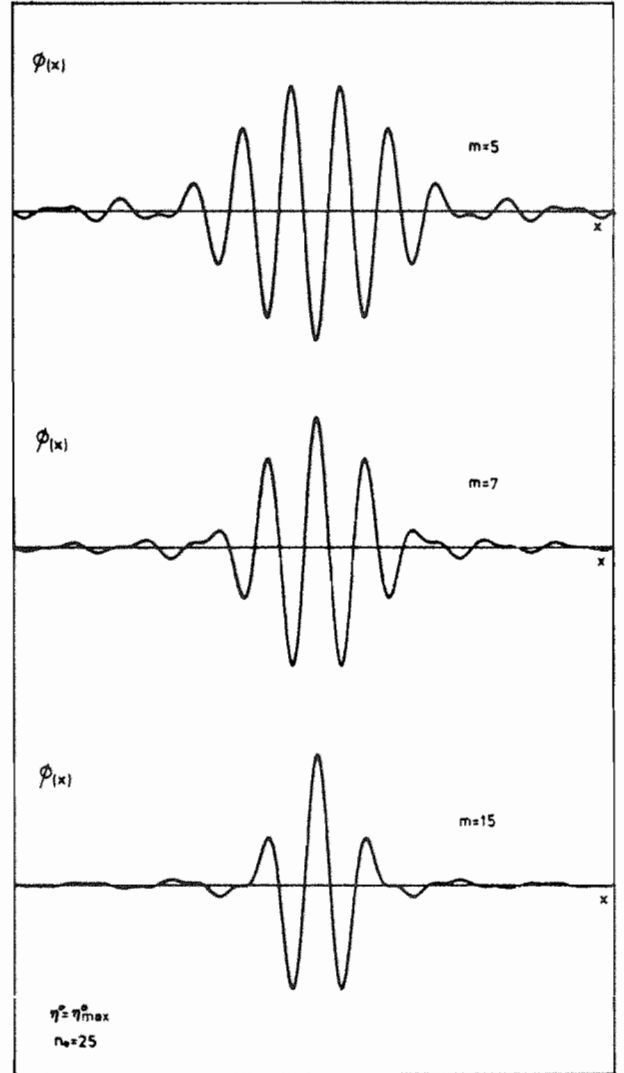


Fig. 2 Simply supported beam: localization along path of steepest descent.

the second approximation level. We shall consider three different problems, namely, a simply supported beam, a fixed-free beam, and a fixed-supported beam. Two more cases characterized by no single interaction are treated in Ref. 18.

In Table 1, the coefficients c_{1jk} , c_{122} , and c_{1jk}^* defined by Eqs. (20) and (30b) are derived under the hypothesis that $n_j, n_k \gg 1$. Note that because of this simplifying assumption, these coefficients are independent of the middle value of the set of n_j .

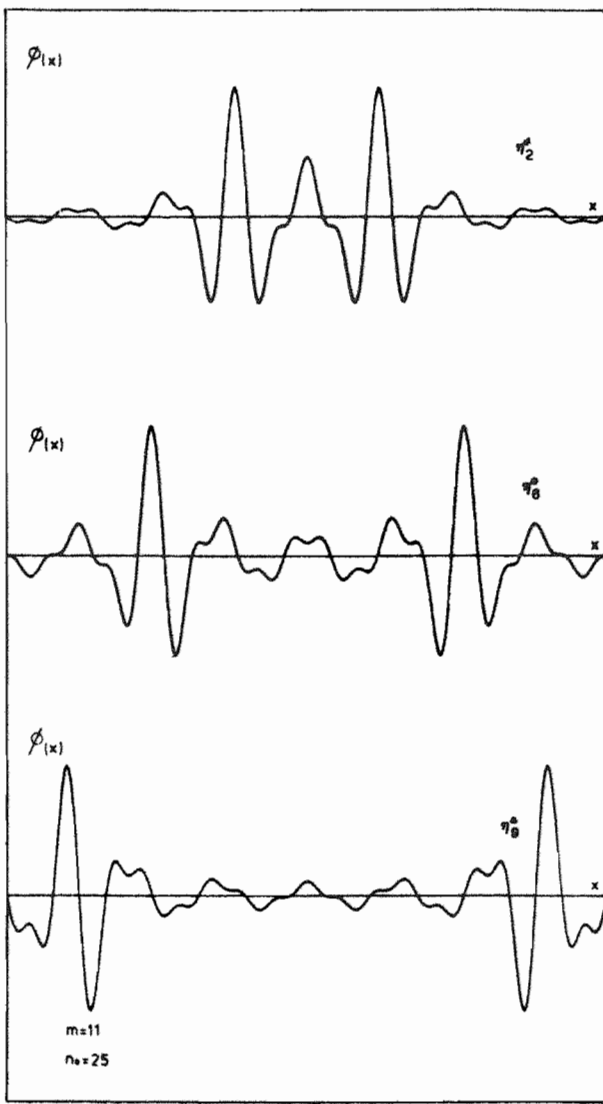


Fig. 3 Simply supported beam: localization along different bifurcated paths.

For the three beams, Eq. (29) has been solved for increasing values of m , and it is found that the eigenvalues of the first two cases coincide. The values of η_{\max}^* vs m have been plotted in Fig. 1, where it is apparent that the amplifying effect due to multiple interaction is much larger for the fixed-supported beam in comparison with the other two. For increasing values of m , η_{\max}^* rapidly approaches the asymptote $\pi/2$ for the first two beams and 3.69 for the third. Correspondingly, η_{\min}^* approaches zero and -3.60 , respectively. For increasingly large values of m , there is an infinite number of bifurcated paths, with amplifying factors ranging between η_{\min}^* and η_{\max}^* . Note that the sign of η^* is in accordance with the sign of $f''(x)$, as was discussed at the end of the previous section.

Let us now consider the x dependence $\phi(x)$ of the lateral displacement due to local buckling. Figure 2 shows the local deflection $\phi(x)$ corresponding to the bifurcated path of steepest descent for the simply supported beam in correspondence with different values of m . It is seen that for an increasing number of interacting modes, the deformation tends to localize at midspan. This phenomenon is known in the technical literature as localization of buckling patterns and has been observed experimentally in Ref. 15 and investigated analytically in Refs 16 and 17. In Fig. 3, the local deformations relative to various bifurcated paths corresponding to η_{\max}^* , η_{\min}^* , η_{δ}^* have been represented for a fixed value of m . It is seen that for decreasing values of η^* , localization moves toward the ends of the beam.

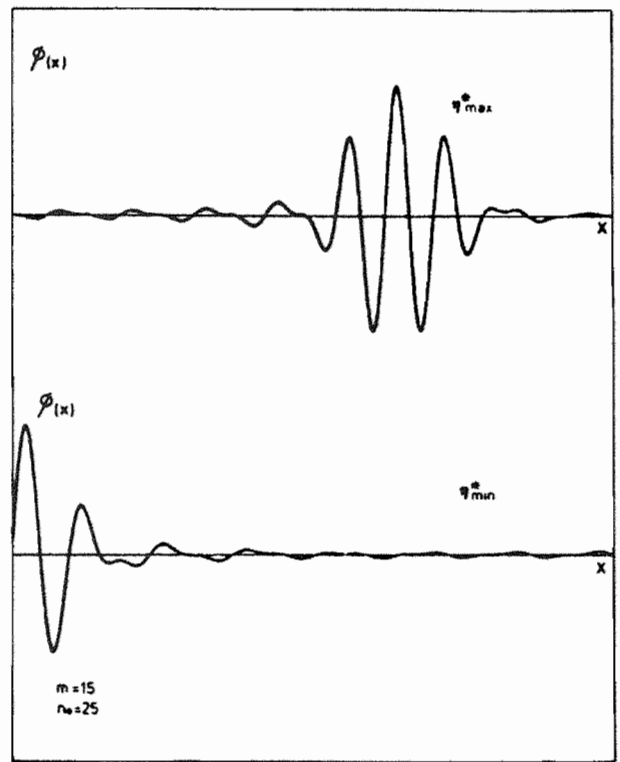


Fig. 4 Fixed-supported beam: localization along paths of maximum positive and negative slope.

Quite analogous is the behavior of the fixed-supported beam. In Fig. 4, the localization is represented in correspondence with η_{\max}^* and η_{\min}^* . It is observed that for $\eta^* = \eta_{\max}^*$, the deformation is concentrated around the point of maximum bending moment ($x/\ell = 0.601$), and for $\eta^* = \eta_{\min}^*$, localization occurs at the fixed end, where there is the largest negative moment. For intermediate values of η^* , one may have a single localization for $\eta^* < 0$ or two localizations for $\eta^* > 0$.

V. Continuum Representation for an Infinite Number of Local Buckling Modes

Results so far obtained show that for a sufficiently large number m of interacting local buckling modes, 1) η_{\max}^* and η_{\min}^* approach an asymptote; 2) there are $2m$ bifurcated paths with amplifying factors ranging between η_{\max}^* and η_{\min}^* ; and 3) the local lateral displacement localizes in different sections of the TWM according to the value of η^* .

These results can be justified on the basis of a continuum representation that consists of replacing the algebraic Eqs. (29) with a differential eigenvalue problem. To this end, let us consider the differential equation

$$\{[f''(x) - \beta]\phi'(x)\}' = 0 \quad (31)$$

where $f(x)$ is the function defined by Eqs. (16), $\phi(x)$ is the unknown function that must satisfy the boundary conditions

$$\phi(0) = \phi(\ell) = 0 \quad (32)$$

and β is the eigenvalue. Let us solve the differential equation by means of a Galerkin procedure by assuming for $\phi(x)$ the series expansion

$$\phi(x) = \sum_{j=2}^{m+1} \frac{v_j}{n_j} \sin n_j \frac{\pi x}{\ell} \quad (33)$$

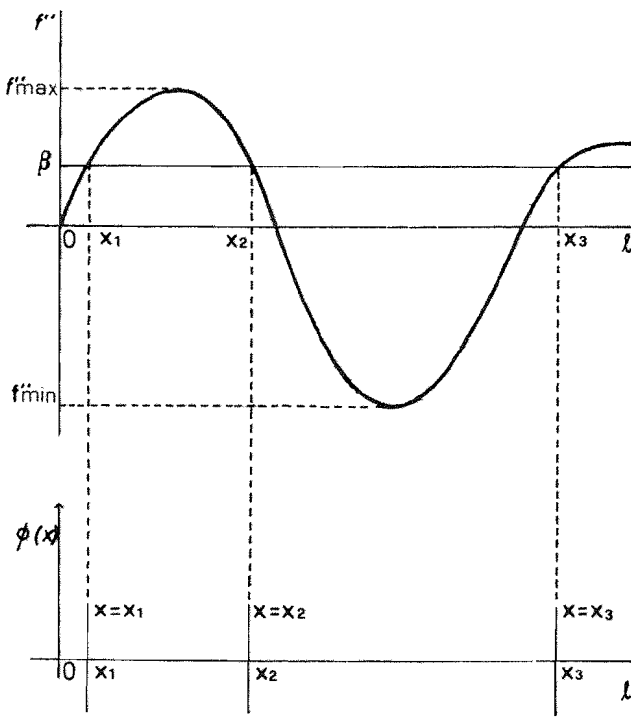


Fig. 5 Singular solutions of Eq. (31).

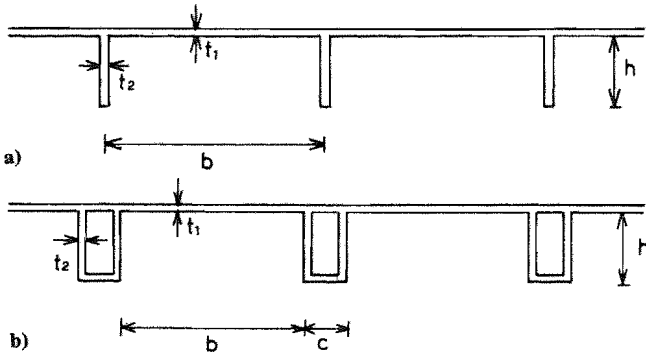


Fig. 6 Stiffened panels: a) slender stiffeners; b) stocky stiffeners.

which satisfies the required boundary conditions for any value of the arbitrary coefficients v_j . By replacing Eq. (33) into the variational principle

$$\int_0^{\ell} [(f'' - \beta)\phi]' \delta\phi \, dx = 0 \quad (34)$$

integrating by parts, and using Eqs. (20) and (30b) one gets

$$[c_{1jk}^* - (\beta\ell/2c_{122})\delta_{jk}]v_j = 0 \quad (35)$$

From comparison of the discrete eigenvalue problems of Eqs. (29) and (35), the relation

$$\eta^* = (\beta\ell/2c_{122}) \quad (36)$$

is obtained. The result, Eq. (36), shows that, for m approaching infinity, η^* can be obtained from the solution β of the continuous problem Eq. (31). Note that, according to Eq. (33), function $\phi(x)$ represents the local displacement.

The continuous problem allows infinite singular solutions for $f''_{\min} \leq \beta \leq f''_{\max}$, which can be interpreted as localization of the function $\phi(x)$. For each value of β , one or more eigensolu-

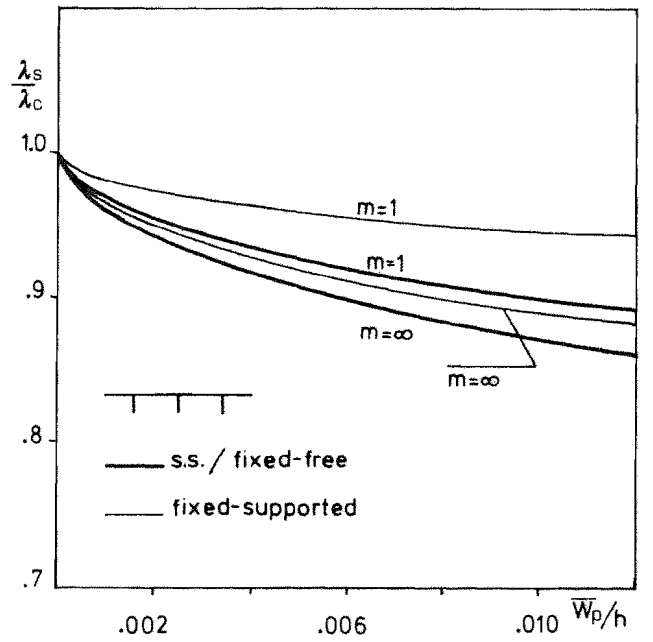


Fig. 7 Sensitivity to initial imperfections for panel with slender stiffeners.

tions $x = x_i$ are obtained for $f''(x_i) = \beta$. Figure 5 illustrates the situation for a given $f''(x)$.

From Eq. (36), the largest positive and negative slopes of the bifurcated paths are obtained:

$$\eta_{\min}^* = \frac{1}{2} \frac{f''_{\max}}{f''_{\min}} (\ell/c_{122}) \quad (37)$$

where η_{\max}^* (η_{\min}^*) is associated with f''_{\max} (f''_{\min}) for a positive value of c_{122} . From Eqs. (37), the path of steepest descent can be determined. The corresponding localization occurs at the cross-section of the largest bending moment in the overall buckling.

Equation (37) may be used for practical purposes for any boundary condition simply by knowing the bending moment function $f''(x)$ due to overall buckling, without any need for solving the linear eigenvalue problem, Eq. (29). Previous results in Sec. IV can be explained in the light of the preceding discussion. Details are given in Ref. 18.

VI. Numerical Results

As an application of the theory presented, we analyze the postbuckling behavior of two stiffened panels with different boundary conditions, the geometry of which is shown in Fig. 6. Panels a and b are characterized by stiffeners with low and high torsional rigidity, respectively. The dimensions are the following: $h = 10$ cm, $b = 30$ cm, and $t_1 = 0.2$ cm for both cases; $t_2 = 0.3$ cm and $\ell_0 = 715$ cm for case a; and $t_2 = 0.2$ cm, $c = 5$ cm, and $\ell_0 = 680$ cm for case b, ℓ_0 being the distance between two consecutive nodal lines in the overall mode.

In the first case, it is assumed that in the local buckling, single plates are simply supported at the joints and buckle according to a sinusoidal law in the transverse direction, while stiffeners rotate rigidly around the junction lines. In the second case, it is assumed that stiffeners do not rotate, and, therefore, plates are fixed along the longitudinal edges. The geometry has been selected in such a way that Euler and local buckling occur simultaneously.

In order to perform postbuckling analysis, we first note that, due to the high value of the aspect ratio ℓ_0/b , lateral deflection of a single plate in the local buckling is practically independent of the number of longitudinal half-waves n_j for

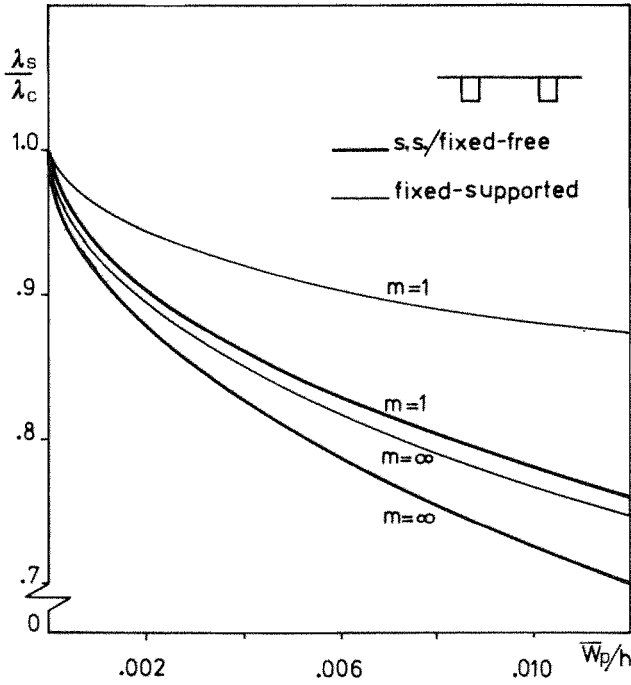


Fig. 8 Sensitivity to initial imperfections for panel with stocky stiffeners.

both panels, and, therefore, the second approximation level of the theory can be applied.

A. Panel with Slender Stiffeners

According to the selected geometry, it is found that the critical stress λ_c is equal to 33.2 MPa. The lateral local displacement is given by

$$W_c(y) = \sin \frac{\pi y}{b} \quad (38a)$$

on the plate

$$W_c(y) = \frac{\pi}{b} y \quad (38b)$$

on the stiffener. The overall longitudinal displacement is furnished by

$$U_1(y) = d \quad (39a)$$

on the plate

$$U_1(y) = d - y \quad (39b)$$

on the stiffener where $d = 1.67$ cm is the distance between the panel centroid and the plate middle plane. By replacing Eqs. (38) and (39) into Eq. (28), the constant \mathcal{A} is obtained:

$$\mathcal{A} = -\frac{Ea_1}{\lambda_c \ell} \left[t_1 db + \pi^2 t_2 \frac{h^3}{b^2} \left(\frac{2}{3} d - \frac{h}{2} \right) \right] \left/ \left(t_1 \frac{b}{2} + \frac{\pi^2}{3} t_2 \frac{h^3}{b^2} \right) \right. \quad (40)$$

By using coefficients c_{122} from Table 1, the values of $\eta_0 = \mathcal{A} c_{122}$ can be determined, and then the slope $\mu = \mu_0$ relative to the single interaction can be evaluated according to

$$\mu_0 = h \frac{\eta_0}{a_1} \quad (41)$$

Equation (41) has been obtained from Eqs. (14) and (23) by selecting as P a corner point (with no local displacement)

belonging to the cross section of largest deflection. The results are $\mu_0 = -0.259$ for a panel simply supported at the ends, $\mu_0 = 0.259$ for a fixed-free panel, and $\mu_0 = -0.081$ for a fixed-sliding panel. By multiplying μ_0 by the limit value of the amplifying factor η_{\max}^* , the actual slope μ corresponding to multiple interaction is obtained. It is found that $\mu = -0.407$, $\mu = 0.407$, and $\mu = -0.299$ for the three boundary conditions examined. In accordance with the sign of μ and with the fact that in the three cases displacements v_p in Eq. (13) are positive if upward, it is found that the load along the equilibrium path decreases for cross-sectional displacements associated with stiffer compression. Figure 7 shows the dependence of the snapping load, Eq. (15), on the initial geometric imperfections amplitude \bar{w}_p/h , both for single ($m = 1$) and multiple interaction ($m = \infty$), and describes the behavior of the simply supported (or fixed-free) and fixed-sliding panel. It is apparent that in both cases, sensitivity to initial imperfections, in passing from single to multiple interaction, increases; the drop of the snapping load for $m = \infty$ and an initial imperfection \bar{w}_p/h around 0.006 is of the order of 10% for the two panels.

B. Panel with Stocky Stiffeners

The critical stress is $\lambda_c = 57.8$ MPa. Since stiffeners do not undergo any lateral displacement or torsional rotation in local buckling, we get, from Eq. (28),

$$\mathcal{A} = -\frac{2Ea_1}{\lambda_c \ell} d \quad (42)$$

with $d = 2.5$ cm, from which, by following previous steps, the slope μ_0 of the postbuckling path is obtained. It is found that $\mu_0 = 1.21$, $\mu_0 = -1.21$, and $\mu_0 = 0.37$ for the three cases of boundary conditions. From μ_0 , the values of μ are derived by multiplying by η_{\max}^* , and the results $\mu = 1.90$, $\mu = -1.90$, and $\mu = 1.36$ are determined. In accordance with the sign of μ , the load along the equilibrium path decreases for cross-sectional displacements associated with panel compression. It is worthwhile to note that panels with stocky stiffeners are more sensitive to initial imperfections than panels with slender stiffeners. This is shown in Fig. 8, where the snapping load in terms of initial imperfections has been plotted. For \bar{w}_p/h around 0.006, there is a reduction of the critical load on the order of 20% for all boundary conditions considered and $m = \infty$. Note that for both panels a and b, curves relative to single interaction are far apart and tend to approach each other for increasing m . This implies that the effect of boundary conditions is softened by the simultaneous occurrence of many buckling modes.

VII. Conclusions

In this paper, the effect of the interaction between one overall and several local buckling modes on the postbuckling of long TWM with asymmetric behavior and various boundary conditions has been analyzed by means of the general theory of stability. Initial geometric imperfections are taken into account.

Under suitable simplifying assumptions, the governing nonlinear equations are replaced by a linear eigenvalue problem that depends on the boundary conditions only. The solution to this problem furnishes the amplifying factor of the slope of the postbuckling paths, which is found useful in applications. Localization of the lateral deformation is verified whenever a large number of local buckling modes occur simultaneously. All results are justified on the basis of a continuum representation where the algebraic eigenvalue problem is replaced by a differential equation.

As a numerical example, the postbuckling behavior of two stiffened panels with slender and stocky stiffeners and different boundary conditions has been investigated. It is found that the second type of panel is more sensitive to initial imperfections. Furthermore, for both panels, the snapping load vs initial imperfections curves, relative to single interaction, are far apart and tend to approach each other for an increasing

number of interacting modes. This implies that the effect of boundary conditions is smoothed by the simultaneous occurrence of several buckling modes.

References

¹Koiter, W. T., "Over de Stabiliteit van het Elastisch Evenwicht," (in Dutch), Ph.D. Thesis, H. J. Paris, Amsterdam, 1945; English translation as NASA TT F-10, 1957, p. 833, and Air Force Flight Dynamics Lab., Rept. TR 70-25, 1970.

²Budiansky, B., "Theory of Buckling and Post-Buckling Behaviour of Elastic Structures," *Advances in Applied Mechanics*, Vol. 14, edited by C.-S. Yih, Academic, New York, 1974, pp. 1-65.

³Van der Neut, A., "The Interaction of Local Buckling and Column Failure of Thin-Walled Compression Members," *Proceedings of the 12th International Congress of Applied Mechanics*, Springer-Verlag, Berlin, 1969, pp. 389-399.

⁴Koiter, W. T. and Kuiken, G. D. C., "The Interaction Between Local Buckling and Overall Buckling on the Behaviour of Built-Up Columns," Delft, the Netherlands, Rept. WTHD-23, 1971.

⁵Byskov, E. and Hutchinson, J. W., "Mode Interaction in Axially Stiffened Cylindrical Shells," *AIAA Journal*, Vol. 15, July 1977, pp. 941-948.

⁶Hancock, G. J., "Interaction Buckling in I-Section Columns," *Proceedings of the 12th International Congress of Applied Mechanics*, American Society of Civil Engineers, New York, Vol. 107, No. ST1, 1981, pp. 165-179.

⁷Sridharan, S., "Doubly Symmetric Interactive Buckling of Plate Structures," *International Journal of Solids and Structures*, Vol. 19, No. 7, 1983, pp. 625-641.

⁸Sridharan, S. and Benito, R., "Columns: Static and Dynamic Interactive Buckling," *Proceedings of the 12th International Congress of Applied Mechanics*, American Society of Civil Engineers, Vol. 110, No. EM1, 1984, pp. 49-65.

⁹Benito, R. and Sridharan, S., "Mode Interaction in Thin-Walled Structural Members," *Journal of Structural Mechanics*, Vol. 12, No. 4, 1984-85, pp. 517-542.

¹⁰Sridharan, S. and Ali, A., "Interactive Buckling in Thin-Walled Beam Columns," *Proceedings of the 12th International Congress of Applied Mechanics*, American Society of Civil Engineers, Vol. 111, No. EM12, 1985, pp. 1470-1486.

¹¹Pignataro, M., Luongo, A., and Rizzi, N., "On the Effect of the Local-Overall Interaction on the Postbuckling of Uniformly Compressed Channels," *Thin-Walled Structures*, Vol. 3, 1985, pp. 293-321.

¹²Pignataro, M. and Luongo, A., "Asymmetric Interactive Buckling of Thin-Walled Columns with Initial Imperfections," *Thin-Walled Structures*, Vol. 5, 1987, pp. 365-386.

¹³Byskov, E., "Elastic Buckling Problem with Infinitely Many Local Modes," Technical University of Denmark, Lyngby, Denmark, Rept. 327, 1986.

¹⁴Pignataro, M. and Luongo, A., "Multiple Interactive Buckling of Thin-Walled Members in Compression," *Proceedings of the 12th International Colloquium on Stability of Plates and Shell Structures*, Ghent, Belgium, 1987, pp. 235-240.

¹⁵Moxham, K. E., "Buckling Tests on Individual Welded Steel Plates in Compression," Cambridge University, Cambridge, England, U.K., Engineering Dept. Rept. CUED/C-Structures/TR3, 1971.

¹⁶Tvergaard, V. and Needleman, A., "On the Localization of Buckling Patterns," *Journal of Applied Mechanics*, Vol. 47, 1980, pp. 613-619.

¹⁷Potier-Ferry, M., "Wavelength Selection and Pattern Localization in Buckling Problems," *Cellular Structures in Instability Problems, Lecture Notes in Physics*, edited by J. E. Wesfreid, and S. Zalesky, Springer-Verlag, Berlin, 1984.

¹⁸Luongo, A. and Pignataro, M., "Boundary Conditions Effects and Localization Phenomenon in Multiple Interactive Buckling of Long Thin-Walled Members in Compression," Università di Roma "La Sapienza," Dipartimento di Ingegneria Strutturale e Geotecnica, Rome, Italy, Rept. 4, 1987.